The Role of Azimuthal Prestress in the Longitudinal Degradation of Nb3Sn Superconducting Magnets

FERMILAB-PUB-24-0947-TD

DOI: 10.1109/tasc.2024.3519079

Fermilab Accepted Manuscript

The Role of Azimuthal Prestress in the Longitudinal Degradation of Nb_3Sn Superconducting Magnets

G. Vallone, G. Ambrosio, E. Anderssen, P. Ferracin

***Abstract*—Superconducting magnet coils are subject to enormous electro-magnetic forces which push the cables away from the winding pole, and against the surrounding structure. This structure is usually optimized trying to limit the overall motion and the strains experienced by the superconducting elements. To achieve this, preload forces are applied both in the coil cross-section and along its length. If the e.m. forces overcome these preloads, separation between the coil and the pole occurs, resulting in an overall loss of rigidity. During the magnet design process, it is often tempting to treat the optimization of the azimuthal and longitudinal preload systems separately. However, the two are inextricably related: as the cross-section preload increases, friction can prevent any motion in the longitudinal plane, and decreasing it can instead allow dangerous motions in the conductor ends. The latter can result in very high strains and, in Nb_3Sn conductors, damage that can prevent the magnet to reach the desired performances. In an attempt to define design guidelines, in this paper we use simplified numerical models to compute, as a function of the in-plane prestress, the variation of the peak strains in the end region of the coils. Finally, we investigate the impact of the azimuthal prestress on a real magnet case, the High-Luminosity Nb_3Sn Quadrupole MQXF.**

***Index Terms*—Mechanical Aspects, Accelerator Magnets, Preload, Nb_3Sn**

I. Introduction

LONGITUDINAL support systems are used in superconducting magnets to contain motions and high strains potentially introduced by the e.m. forces. Existing designs mostly gravitate around two separate approaches: in one, an end-plate is connected to very rigid components, as for example the magnet yoke or an outer stainless steel shell. This design approach, often used in NbTi magnets, seems to be preferred for collared Nb_3Sn magnets [1]. The design philosophy is coherent: both involve a displacement constraint, in one case on the radial surface by the collar, on the other on the coil end by the end plate. An alternative approach, first introduced in [2], attempts instead to introduce a prestress with longitudinal rods, which is generally further increased by differential thermal contraction effects during the cooldown. This solution was proposed as a natural extension of the bladder & key technology [3], which, similarly, allows to control the azimuthal force provided to the coil pack. Some authors also suggested a mixed approach, where longitudinal rods are used to provide a prestress, but with the addition of longitudinal stiffeners to increase the overall stiffness of the system [4].

Automatically generated dates of receipt and acceptance will be placed here
This work was supported by the U.S. Department of Energy, Office of Science, Office of High Energy Physics.

G. Vallone, E. Anderssen and P. Ferracin are with Lawrence Berkeley National Laboratory, Berkeley, CA 94720 USA (e-mail: gvallone@lbl.gov).
G. Ambrosio is with Fermi National Accelerator Laboratory, Batavia, IL 80510 USA.

Colour versions of one or more of the figures in this paper are available online at http://ieeexplore.ieee.org.
Digital Object Identifier: xx

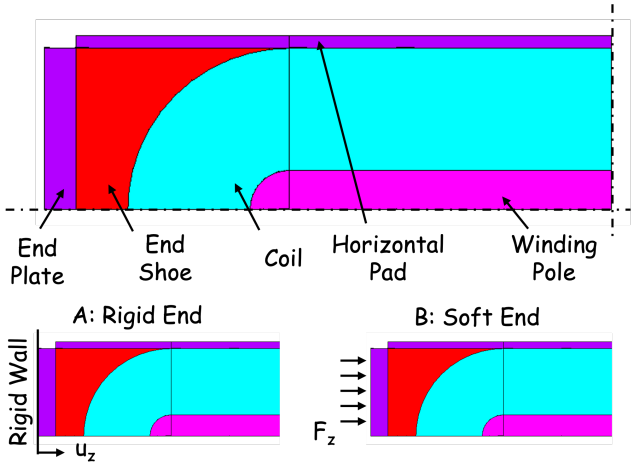

Fig. 1. Top view of the race track model (top), and boundary conditions for the two load cases investigated (bottom).

Both motions and longitudinal strains are considered a potential source of reduction in electro-magnetic performances, capable of introducing training quenches [5]–[7] or damage in the superconducting coils [8], [9]. However, these effects might not only be controlled by the longitudinal system, but also by the amount of prestress applied in the cross-section plane. For example, frictional effects absorb more than 90% of the longitudinal e.m. forces in some magnets [10].

In this paper, we explore the relationship between in-plane prestress and the longitudinal strains induced in superconducting coils. Our investigation begins with abstract numerical models and is subsequently extended to a real magnet case.

II. A Racetrack Model

A. Modeling Assumptions

A simple racetrack model was developed to quickly investigate the peak longitudinal strain computed at the conductor as a function of the applied azimuthal and longitudinal prestress. The 3D model, shown in Fig. 1, includes a Nb_3Sn superconducting coil, wound around a titanium pole, and bounded at the end by a bronze end shoe. Thin stainless steel horizontal and vertical pads surround the coil, and an end plate supports the end of the coil. Rigid boundary conditions are applied at the outer surfaces of the pads, and the components interfaces are modeled using frictional contacts with separation allowed. The

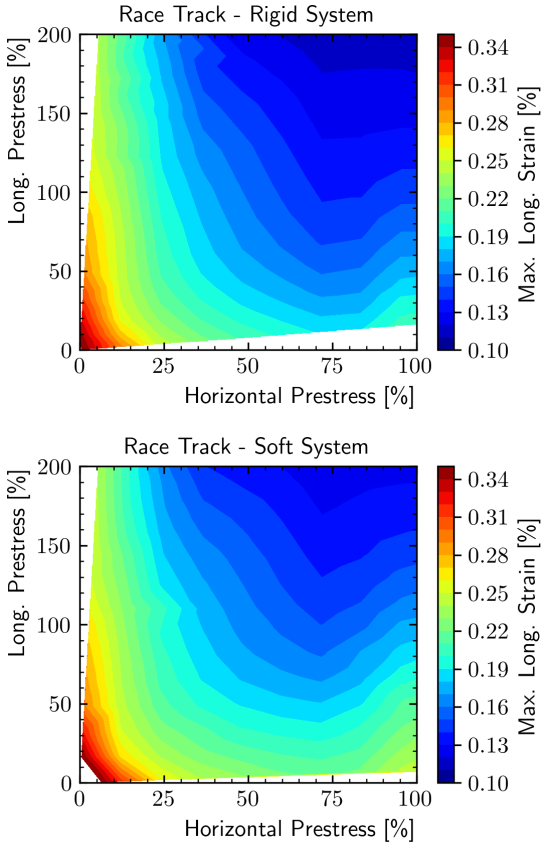

Fig. 2. Peak longitudinal strain computed on the race track model as a function of the azimuthal and longitudinal prestress, expressed as percentage of the respective e.m. force: (top) rigid end model, and (bottom) soft end model.

frictional coefficient is equal to 0.2. The computation includes two steps: a 'prestress' step, and a powering one. In the first step, an interference between the coil, the end shoe and the horizontal pad is used to introduce the horizontal prestress. Longitudinally, two different conditions are used (see Fig. 1, bottom): a rigid displacement boundary at the end of the end plate, and a constant pressure with no constraints. The first one tries to replicate the 'rigid' system typical of collared structures, while the second one the 'rods' system employed in B&K magnets. For simplicity, no cooldown is considered in this simulation. In reality, the coil design might significantly affect the amount of longitudinal prestress that can be provided by the system, for example because of the thermal contraction of the structure (for rigid systems) or of the winding pole for both systems.

B. Parametric Study

A parametric analysis was used to investigate the peak coil longitudinal strain during powering in the azimuthal and longitudinal prestress space. The results, shown in Fig. 2, are very similar for the two prestress systems considered, with similar worst and best conditions achievable, and peak strains always located on the pole turn. Interestingly, the optimal region seems slightly larger for the rigid system. The optimal azimuthal prestress seems to be within a region with 70/80% of the e.m. forces. Larger prestresses affect negatively this result as Poisson's effects start to dominate the overall strain. Similarly, the Poisson's effect introduces 'white' regions in the plot, where the longitudinal prestress introduces an azimuthal one and vice-versa. This does not happen for the soft longitudinal system, which allows a zero longitudinal prestress even with high horizontal prestress levels. On the other hand, because of the very large friction introduced by the azimuthal prestress, the minimum longitudinal strain is reached with a longitudinal prestress larger than the e.m. forces: the optimal value is reached above 150% of the nominal longitudinal force. The model shows how there is a strong interaction between the two systems: it is not possible to minimize the longitudinal strain just by increasing the longitudinal prestress.

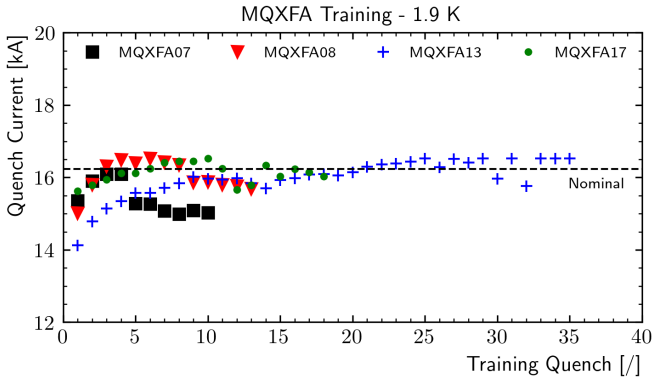

Fig. 3. Training curves of MQXFA07, A08, A13 and A17. Only the quenches at 1.9 K, with the nominal ramp rate, are shown. All the magnets experienced a de-training with quenches in the magnet lead end region.

III. A Real Case: the MQXFA Magnets

MQXF [11] is the low-β quadrupole for the High Luminosity LHC upgrade. The magnets are being built, in two different length, in Europe (MQXFB [12]) and in the US (MQXFA [13], [14]), within the US Accelerator Upgrade Program. The magnet target a nominal field gradient of 132.6 T/m within a 150 mm coil aperture. The peak field at nominal field is around 11.4 T. The mechanical design employs bladder & keys to provide the azimuthal prestress at room temperature, with an aluminum shell to further increase it during cooldown to cryogenic temperature; and an end-plate and rod longitudinal system to apply the longitudinal prestress. This system is equivalent to the soft system presented in Section II.

By design, a full (100% of the e.m. forces, equal to 1.2 MN per magnet end) prestress is provided at cold by the longitudinal system. A study of the impact of these forces on the contact conditions in the ends was provided in [10], where it was also shown that most of the e.m. force is in reality absorbed not by the rods, but by the friction introduced by the loading keys.

During the MQXFA series production [15], 12 successful magnets were built [16]. However, 4 magnets (A07, A08, A13 and A17) failed to meet the required performances. These magnets, whose training curve is shown in Fig. 3, showed a sudden de-training after few training quenches. Quench

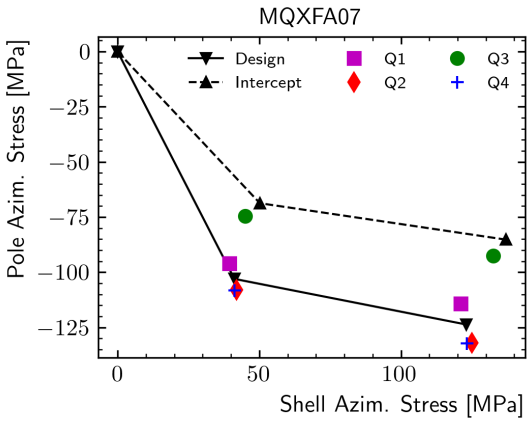

Fig. 4. Computed prestress on a full non-symmetric model of the MQXFA07 magnet. The undesired interception of the prestress by the pole key reduces the prestress in the coil in quadrant 3 (Q3).

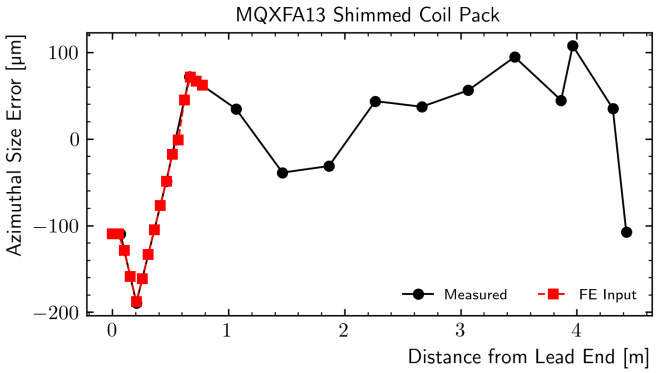

Fig. 5. Azimuthal coil pack size error, after shimming, for MQXFA13: from coil size measurements, and as used in the end region FE model. The size is uniform in the straight section, with a sudden drop in the lead end region.

antenna data showed that these quenches were all occurring in the lead end region of the magnet. A through investigation of the causes was started, which pointed at potential unwanted reductions of the azimuthal prestress with respect to the design value.

A. Azimuthal Prestress Non-Conformities

The magnet specifications provides strict constraints on the applied azimuthal prestress applied at room temperature, balancing the need to provide sufficient support to the coils, and to avoid damaging them during the preload operations. However, in magnets MQXFA07 and A08 [15], [17], asymmetric assembly conditions caused interception of part of the prestress by a structural element (the pole keys, see [18]). A computation on non-symmetric models of the magnet, with results reported in Fig. 4 for A07, predicted a 25 MPa reduction of the 'average' prestress applied on the quadrant 3 coil, the limiting one.

On the other hand, MQXFA13 and MQXFA17 coil pack sizes, reported in Fig. 5, seemed to be smaller than average in the limiting region, the lead end. An analytical model [19] allows to compute an expected prestress change due to coil

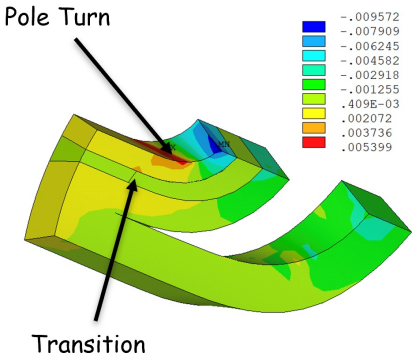

Fig. 6. Longitudinal strain, in m/m, in the lead end of the quadrant 3 coil for the MQXFA07 magnet. Two critical regions are identified: the wedge/end-spacer transition, and the pole turn.

size of 27 MPa for a 100 μm size variation [19]. Locally, this would mean a reduction of about 65 MPa at the worst point (250 μm) for both magnets.

B. Coil End Region Strain

Detailed FE models of all the non-conforming magnets were used to compute the strain in the end-region. To reduce the computational burden, the simulation included only the end regions of the magnet, as shown in Fig. 5. The coils were assumed to be detached from the winding pole. The analysis showed also significant tension (>20 MPa) at the interface between the inner coil wedge and end-spacer, which was subsequently left open.

The models pointed at two potential damage locations in the coils with a lower average (A07 or A08) and local (A13, A17) prestress: the pole turn, and the wedge/end-spacer transition. Metallurgical inspections performed on the limiting coils revealed several several cracked filaments at both sides of the wedge/end-spacer transition [15], [20].

IV. Practical Solutions

A. Global Prestress

As in the race track model, the conductor longitudinal strain can be reduced by increasing the overall azimuthal prestress applied. During the assembly procedure, the amount of prestress applied is checked against strain measurements on the winding pole. Fig. 7 shows the relationship between this measurement after the assembly operations, and the predicted peak longitudinal strain during powering. In the nominal case, with coils with uniform coil size, the inverse dependence is mostly linear up to a non-linearity, appearing at 70 MPa, which introduces larger variations of strain as a function of prestress variations. A 'strain' limit can then be used to define a minimum prestress required.

In A07 and A08 the overall unbalance in prestress introduced by the unwanted interception was solved with improved assembly procedures [17], allowing to bring back the prestress level to the desired value. With these solutions, and after changing the limiting coils, the magnet was able to reach the desired performances.

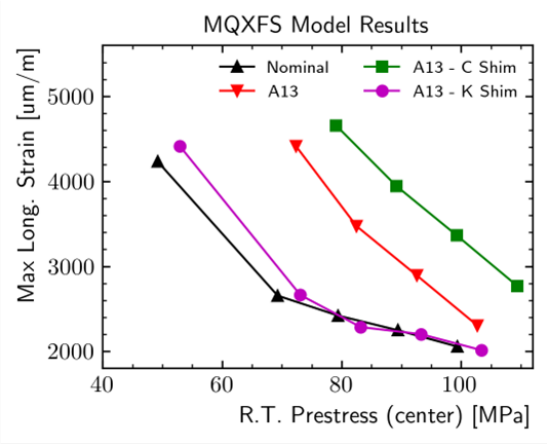

Fig. 7. Peak longitudinal strain as a function of the room temperature azimuthal prestress for a nominal coil pack and considering the MQXFA13 coil size, with and without local prestress modifiers. The value considered for the prestress is the one at the center of the magnet, where strain gauges are installed to monitor the prestress.

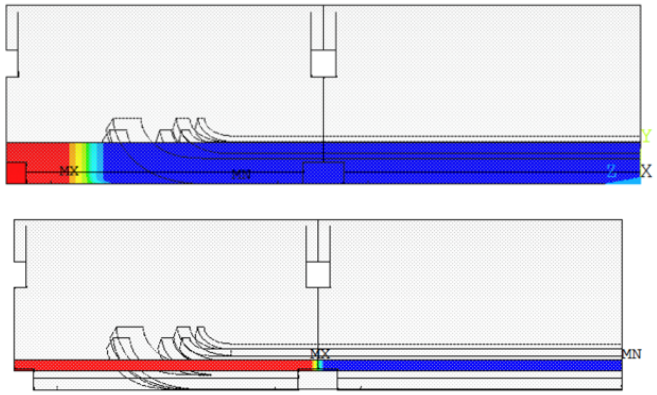

Fig. 8. Modeled interference for local pre-stress modifiers: radial shimming between the coil and the collar (top); and tapered loading key (bottom). The colors represent the relative size of the modeled interference.

B. Local Prestress Modifiers

The overall picture is more complicated when the high strain is due to a local size variation. As shown in Fig. 7 for the A13 magnet, the reduction in coil size in the end significantly increases the peak longitudinal strain reached for the same prestress level. With this constraint, increasing the average prestress can become unfeasible as it might imply excessive stresses in the straight section.

A potential solution is to introduce 'local' prestress modifiers in the magnet assembly. Two different ideas were tested on the numerical models: additional local radial shimming between the coil and the collar; and a local increase in the size of the loading keys. The former is limited by the fact that the available space is relatively short: to avoid 'steps' near the conductor, the shimming can be applied only up to the last coil turn (Fig. 8, top). The latter leaves, instead, more freedom. For example, it would allow to increase the loading key thickness along a whole shell (8, bottom).

The impact of both modifications on the coil strain is

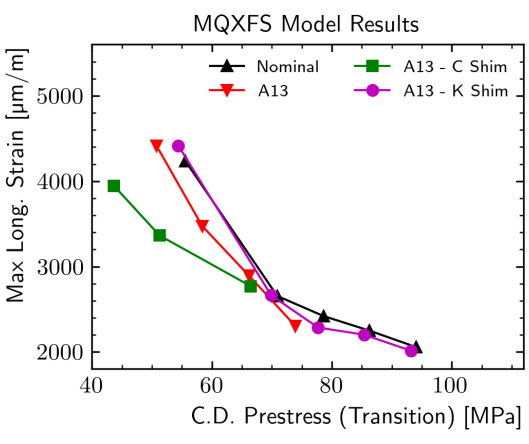

Fig. 9. Peak coil longitudinal strain as function of the azimuthal prestress applied at the wedge/end spacer transition location after cooldown.

reported in Fig. 7: while the collar shim (C-Shim) goes in the wrong direction, further increasing the strain, the loading key (K-Shim) allows to remove completely the danger due to undersized coil ends. The peak longitudinal strain seems to be mostly related to the local azimuthal prestress provided after cooldown at the transition region, as shown in Fig. 9 for all the considered cases. This explains the different effectiveness of the two approaches: there are no constraints on the magnet portion covered by the increased loading key shim size, allowing to cover the critical transition area; instead, the collar shim space is limited to the end-shoe region, far from where the prestress increase is needed. A tapered loading key shim was introduced in the lead end region of the A18 magnet: no quenches occurred in this region, and the required performances were successfully met [16].

V. Conclusion

The peak longitudinal strain experienced by coils during powering seems to be inextricably affected by the level of cross-sectional prestress provided by the magnet support structure. Simplified numerical models show that this relationship does not depend on the type of longitudinal support system used, as long as the coils are provided with sufficient prestress in both the horizontal/azimuthal and longitudinal directions. Results also suggest that, at least for the case considered, a minimum in the longitudinal strain is reached for an azimuthal prestress equal to 80% of the e.m. forces.

An undesired reduction of azimuthal prestress was also identified as a critical cause behind the unsatisfactory performances of 4 MQXFA magnets. Numerical models pointed to very high longitudinal strains at the wedge/end-spacer transition. Metallurgical inspections confirmed the presence of several broken filaments in this area. The prestress reduction was, depending on the magnet, global or local in nature: solutions were presented for both cases. An improvement of the assembly procedures allowed to address the global reduction, as already tested successfully on two magnets. Local modifiers are being applied to in-production magnets: the first magnet tested with an increased loading key thickness in the end region yielded the required performances.

REFERENCES

[1] F. Savary *et al.*, "Design, assembly, and test of the CERN 2-m long 11 T dipole in single coil configuration," *IEEE Transactions on Applied Superconductivity*, vol. 25, no. 3, pp. 1–5, 2015.

[2] P. Ferracin *et al.*, "Mechanical analysis of the Nb_3Sn dipole magnet HD1," *IEEE Transactions on Applied Superconductivity*, vol. 15, no. 2, pp. 1119–1122, 2005.

[3] S. Caspi *et al.*, "The use of pressurized bladders for stress control of superconducting magnets," *IEEE Transactions on Applied Superconductivity*, vol. 11, no. 1, pp. 2272–2275, 2001.

[4] G. Vallone *et al.*, "3D mechanical analysis of a compact Nb_3Sn IR quadrupole for EIC," *IEEE Transactions on Applied Superconductivity*, vol. 31, no. 5, pp. 1–5, 2021.

[5] P. Ferracin *et al.*, "Mechanical design of HD2, a 15 T Nb_3Sn dipole magnet with a 35 mm bore," *IEEE Transactions on Applied Superconductivity*, vol. 16, no. 2, pp. 378–381, 2006.

[6] P. Ferracin and S. Caspi, "Finite element model of training in the superconducting quadrupole magnet SQ02," *Cryogenics*, vol. 47, no. 11, pp. 595–606, 2007, CHATS on Applied Superconductivity 2006.

[7] G. Vallone *et al.*, "Modeling training in Nb_3Sn superconducting magnets," *IEEE Transactions on Applied Superconductivity*, vol. 34, no. 5, pp. 1–5, 2024.

[8] N. Cheggour, T. C. Stauffer, W. Starch, L. F. Goodrich, and J. D. Splett, "Implications of the strain irreversibility cliff on the fabrication of particle-accelerator magnets made of restacked-rod-process Nb_3Sn wires," *Scientific Reports*, vol. 9, no. 1, pp. 1–14, 2019.

[9] B. Bordini, P. Alknes, L. Bottura, L. Rossi, and D. Valentinis, "An exponential scaling law for the strain dependence of the Nb_3Sn critical current density," *Superconductor Science and Technology*, vol. 26, no. 7, p. 075 014, 2013.

[10] G. Vallone *et al.*, "Mechanical design analysis of MQXFB, the 7.2 m long low- β quadrupole for the High-Luminosity LHC upgrade," *IEEE Transactions on Applied Superconductivity*, vol. 28, no. 3, pp. 1–5, 2018.

[11] P. Ferracin *et al.*, "The HL-LHC low-β quadrupole magnet MQXF: From short models to long prototypes," *IEEE Transactions on applied superconductivity*, vol. 29, no. 5, pp. 1–9, 2019.

[12] S. I. Bermudez *et al.*, "Progress in the development of the Nb_3Sn MQXFB quadrupole for the HiLumi upgrade of the LHC," *IEEE Transactions on Applied Superconductivity*, vol. 31, no. 5, pp. 1–7, 2021.

[13] G. Ambrosio, "US HL-LHC Accelerator Upgrade Project (MQXFA final design report)," Lawrence Berkeley National Lab.(LBNL), Berkeley, CA (United States …, Tech. Rep., 2022.

[14] G. Ambrosio *et al.*, "Lessons learned from the prototypes of the MQXFA low-beta quadrupoles for HL-LHC and status of production in the US," *IEEE Transactions on Applied Superconductivity*, vol. 31, no. 5, pp. 1–5, 2021.

[15] G. Ambrosio *et al.*, "Challenges and lessons learned from fabrication, testing, and analysis of eight MQXFA low beta quadrupole magnets for HL-LHC," *IEEE Transactions on Applied Superconductivity*, vol. 33, no. 5, pp. 1–8, 2023.

[16] G. Ambrosio, *Private communication*, 2024.

[17] D. W. Cheng *et al.*, "The challenges and solutions of meeting the assembly specifications for the 4.5 m long MQXFA magnets for the Hi-Luminosity LHC," *IEEE Transactions on Applied Superconductivity*, vol. 33, no. 5, pp. 1–5, 2023.

[18] G. Vallone *et al.*, "Mechanical analysis of the short model magnets for the Nb_3Sn low-β quadrupole MQXF," *IEEE Transactions on Applied Superconductivity*, vol. 28, no. 3, pp. 1–6, 2018.

[19] G. Vallone *et al.*, "Summary of the mechanical performances of the 1.5 m long models of the Nb_3Sn low-β quadrupole MQXF," *IEEE Transactions on Applied Superconductivity*, vol. 29, no. 5, pp. 1–5, 2019.

[20] A. Moros *et al.*, "A metallurgical inspection method to assess the damage in performance-limiting Nb_3Sn accelerator magnet coils," *IEEE Transactions on Applied Superconductivity*, vol. 33, no. 5, pp. 1–8, 2023.